TÜBİTAK

Turkish Journal of Physics

http://journals.tubitak.gov.tr/physics/

Research Article

Turk J Phys
(2022) 46: 239 – 251
© TÜBİTAK
doi:10.55730/1300-0101.2730

3D self-assemble formation of molybdenum disulfide (MoS_2)-doped polyacrylamide (PAAm) composite hydrogels

Sümeyye DURMAZ, Ekrem YILDIZ, Bengü Özuğur UYSAL*, Önder PEKCAN
Faculty of Engineering and Natural Sciences, Kadir Has University, İstanbul, Turkey

Received: 10.11.2022 • **Accepted/Published Online:** 21.12.2022 • **Final Version:** 27.12.2022

Abstract: Polyacrylamide (PAAm), a renowned member of the hydrogel class, has many uses throughout a wide range of industrial processes, including water absorbed diapers, contact lenses, wastewater treatment, biomedical applications such as drug delivery vehicles and tissue engineering because of its physical stability, durability, flexibility easier shaping, and so on. PAAm also provides new functionalities after the incorporation of inorganic structures such as molybdenum disulfide (MoS_2). During the copolymerization process, the transmittance of all samples reduced significantly after a particular time, referred to as the gel point. Microgels form a tree above the gel point as projected by Flory-Stockmayer classical theory. Because of microgels positioned at the junction points of the Cayley tree, the addition of MoS_2 results in strong intramolecular crosslinking and looser composites. Moreover, fractal geometry provides a quantitative measure of randomness and thus permits characterization of random systems such as polymers. Fractal dimension of these polymer composites is calculated from power-law-dependent scattered intensity. It was also confirmed that a hydrogel rapidly formed within a few seconds, indicating a 3D network formation inside the gel. These materials may have a great potential for application in wearable and implantable electronics due to this highly desired 3D self-assemble feature.

Keywords: MoS_2, 3D self-assemble gelation, optical properties, response rate of composite gel.

1. Introduction

Graphene and transition metal dichalcogenides (disulphides and selenides of molybdenum and tungsten etc.) are two-dimensional (2D) materials and they have been used in the production of energy storage units, opto-electronics, and catalysis [1, 2]. Molybdenum disulphide (MoS_2) is the most important one because of its electronic behavior and mechanical properties [3, 4]. MoS_2 is classified as a semiconductor material because it has a band gap energy of about 1.2 eV. However, the magnitude of this band gap energy is insufficient for many electronic applications [5, 6]. In fact, the minimum band gap energy required for technological applications must be greater than 1.4 eV. Therefore, it is necessary to prepare composites of different materials to provide the desired band gap values of these 2D structures [7]. In addition, it has been thought that MoS_2 has the capacity to increase and regulate mechanical properties when incorporated into basic molecular hydrogels [8, 9]. Since hydrogels have the ability to absorb large amounts of water without dissolving, resulting from their macroscopic scale cross-linked structure between polymer chains, they have a specific elasticity. As a

*Correspondence: bozugur@khas.edu.tr

This work is licensed under a Creative Commons Attribution 4.0 International License.

famous member of hydrogel class, polyacrylamide (PAAm) is an organic polymer. PAAm is preferred as promising hosting organic matrix for composite materials due to its easier shaping, durability, and exceptional processability features; it is produced with a simple, repeating, linear chain structure but can be modified to form highly structured, branched, and cross-linked variants [10]. Besides having optical and mechanical stability, PAAm gains new functionalities with the addition of nanofillers such as molybdenum disulfide (MoS_2). According to the earlier research [11–14], doping with nano-filler materials such as carbon nanotube and graphene oxide has improved the optical, mechanical, and electrical behavior of polystyrene, latex, and PAAm. Polymer composites incorporating MoS_2 are expected to show improved properties as a result of enhanced interfacial compatibility. In addition to the intrinsic properties of the polymer used, a further enhancement of biocompatibility can be made to increase their possessed useful properties of value to in electrochemistry, catalysis, and supercapacitors, which can be achieved by inclusion of molybdenum disulfide (MoS_2) into the polymers [15]. In other studies, it is well-known and numerous attempts have been made in terms of band gap energy studies using UV-Vis spectrometer measurements. However, it is crucial to study the gelation mechanism of the material in order to show different aspects of copolymerization regarding different content of nanofillers. It is also necessary to use fractal geometry to explain this kind of copolymerization process. That is why in this study, the gelation mechanism and fractal dimension of MoS_2-reinforced PAAm are studied. MoS_2 is used as nanofiller to improve the conductivity of the gels. A composite hydrogel rapidly formed within a few seconds, indicating a self-assembled 3D network formation inside the gel. The effect of MoS_2 amount on the gelation mechanism of new composites is crucial for time 3D printing and implantable electronic applications where there is a time constraint to gelling to be very fast and homogenous.

2. Theoretical background

2.1. Light scattering of polymer composites

As is known, Rayleigh scattering refers to the scattering of electromagnetic radiation by particles smaller than their wavelength, λ according to the equation as follows:

$$I_{sc} = k\, c\, \lambda^{-\eta}\, I_0\, \nu^2, \tag{2.1}$$

where I_{sc} is the scattering intensity and I_0 is the incident intensity of the electromagnetic radiation, in this case, light; k contains n_1 and n_0 which are the indices of refraction of the dispersed phase and the dispersion medium like a liquid mixture, solution, respectively; c is the number of particles in 1 cc called numerical concentration; η is the size-dependent power factor, and ν is the volume of one particle. Eq. (2.1) applies only to spherical particles with a small radius compared to the wavelength of the scattered light. As light passes through a liquid mixture, it scatters from structures up to 1/10 of the wavelength, forming opaque regions. These opaque regions also block transparency as the overall appearance. Thus, one can encounter a standard scattering behavior, namely the size-dependent power factor of 4. As another scenario, if the liquid mixture contains structures greater than 10% of the wavelength of the incident light considering the wavelength range of the light being studied (400-700 nm), the term of size-dependent power factor becomes smaller, even falling below 3 so, the intensity of the scattered light changes faster with wavelength [16]. Therefore, it becomes difficult to control the scattering.

2.2. Polymerization process and gel formation

Voyutsky's kinetic model [16] is used for the polymerization process, where the rate of monomer consumption i.e. the rate of polymerization is given by the following equation:

$$\frac{d[M]}{dt} = -k_r\,[M]. \tag{2.2}$$

Here [M] is the concentration of monomer and k_r is the composite rate constant of gelation. The monomer consumption can be written as

$$[M] = [M_0]\,exp(-k_r t) \tag{2.3}$$

where $[M_0]$ is the concentration of monomer at $t = 0$. Throughout the polymerization process, monomer consumption, namely gel formation inside the polymer can be chosen proportional to the transmitted light intensity I_{tr}. The turbidity in the dispersed medium occurs leading to a decrease in I_{tr} when gels form [17]. Over time, monomers combine to contribute to the polymer structure and thus gel formation, while the transmitted intensity of light I_{tr} passing through the polymer decreases exponentially, that is, the scattering intensity increases due to newly formed scattering centers.

$$I_{tr} = exp(-k_r t) \tag{2.4}$$

On the other hand, if it is assumed that the particles are spherical and the volume ν, of these microparticles increases linearly in time, t before gel formation and throughout the gelation, for the scattering intensity values, a linear change with respect to the square of time would be expected according to Eq. (2.1).

The Flory-Stockmayer approach and percolation theory [18–23] based on modeling the sol-gel phase transition can be used to explain the polymerization process. Mean field theory and other statistical theories try to describe polymerization processes formed by functional groups with equal reactivity with tree approaches. In the polymerization process resulting from the combination of monomers, if p is defined as the probability of monomer bonding and p_c is the critical point of this percolation, namely, the gel point, then the gel fraction G has a scaling behavior describing the difference between these two situations and is expressed as:

$$G = A(p - p_c)^{\beta} \qquad p \to p_c \tag{2.5}$$

Here β is the critical exponential term and A is the proportionality factor. In the Flory-Stockmayer approximation, the critical exponential term is 1. In a situation where temperature and concentration are kept constant, probability p will be directly proportional to time t [19, 21, 23]. With scattering intensity, I_{sc} up to the gel point, i.e. $t < t_g$, the mean cluster size of the polymers can be determined. Above t_g, scattering intensity measures the gel fraction G, the fraction of monomers belonging to the macroscopic network.

$$I_{sc} = B\,(t - t_g)^{\text{critical term}} \qquad t \to t_g \tag{2.6}$$

It predicts the Flory-Stockmayer classical theory, i.e. tree approximations during gelation. In other words, structures inside the solution form a tree above the gel point during gel formation [24].

2.3. Fractal dimension calculations

The self-similarity property is characteristic of fractal objects such as long polymer chains. This fractal behavior is unlike that usually associated with solid objects since long molecules exhibit a dynamical fractal property. The dynamical fractal character of a chain in dilute solution is easily perceived from its average dimension, measured from light scattering, for example. Observing the fractal character in a composite gel is more difficult because there is a strong interpenetration of chains. The density of the whole sample is practically constant, regardless of the number of submolecules, whether they are crosslinked or not [25, 26]. For so-called mass fractals (i.e. polymer-like structures) the fractal dimension D, which relates the size R of the object to its mass M [27],

$$M \sim R^{\mathrm{D}} \tag{2.7}$$

It is obvious to interpret that increasing MoS_2 content increases the number of microgel particles, which leads to a decrease in the compactness of the macrogel structure.

3. Experimental details

3.1. Composite gel preparation

All powder chemicals were weighed using Semi-Micro Dual Range Laboratory Balance (DUAL Precisa HA225SM-DR). Firstly, 5 mL of distilled water was taken into a clean beaker by using a pipette. Subsequently, 2.0 g of acrylamide (AAm, Sigma-Aldrich) was weighed and added into the beaker. AAm was dissolved in distilled water and 6.1 mg of polyvinylpyrrolidone (PVP, Sigma-Aldrich) was added into the beaker so as to homogenize the 2D MoS_2 structures inside the gel. Next, 0.5 mg of MoS_2 powder was weighed and added to the solution. After this step, 0.01 g of methylenebisacrylamide and 0.008 g of Ammonium persulfate were weighed by using microscale, and they were added into the beaker. The solution was mixed until all components of mixture were dissolved completely by helping magnetic stirring. Finally, 8 μL of N,N,N',N'-tetramethylethylenediamine (TEMED, Sigma-Aldrich) was added to the beaker as an activator of the reaction. A quartz cuvette was filled with the prepared solution. These experiments were conducted at room temperature (24° C, Humidity: 40%). The whole process was repeated for various MoS_2 contents (1, 1.5, 2, 2.5, 3, 3.5, 4 mg).

3.2. Composite gel characterization

The quartz cuvette with the prepared solution was placed in the measurement cabin. Each solution's transmittance data was measured by using UV-Vis spectrophotometer (Labomed Spectro 22) at 650 nm wavelength. Gelation processes and photon transmission intensities, I_{tr}, were monitored in real time by the camera system. The data was recorded for about 300 s. until the transmittance ratio is being constant.

4. Results and discussion

Data of transmission was measured using a real-time camera. The gelation process was observed using transmission measurement with UV-Vis spectrophotometer at the constant wavelength of 650 nm. Before and after gelation, data was recorded for every 15 s; however, during gelation process, transmission curves were formed using data taken every 3 s in order to calculate the accurate gel point. Next, these sigmoidal curves in Figure 1a are formed. The light intensity passing through

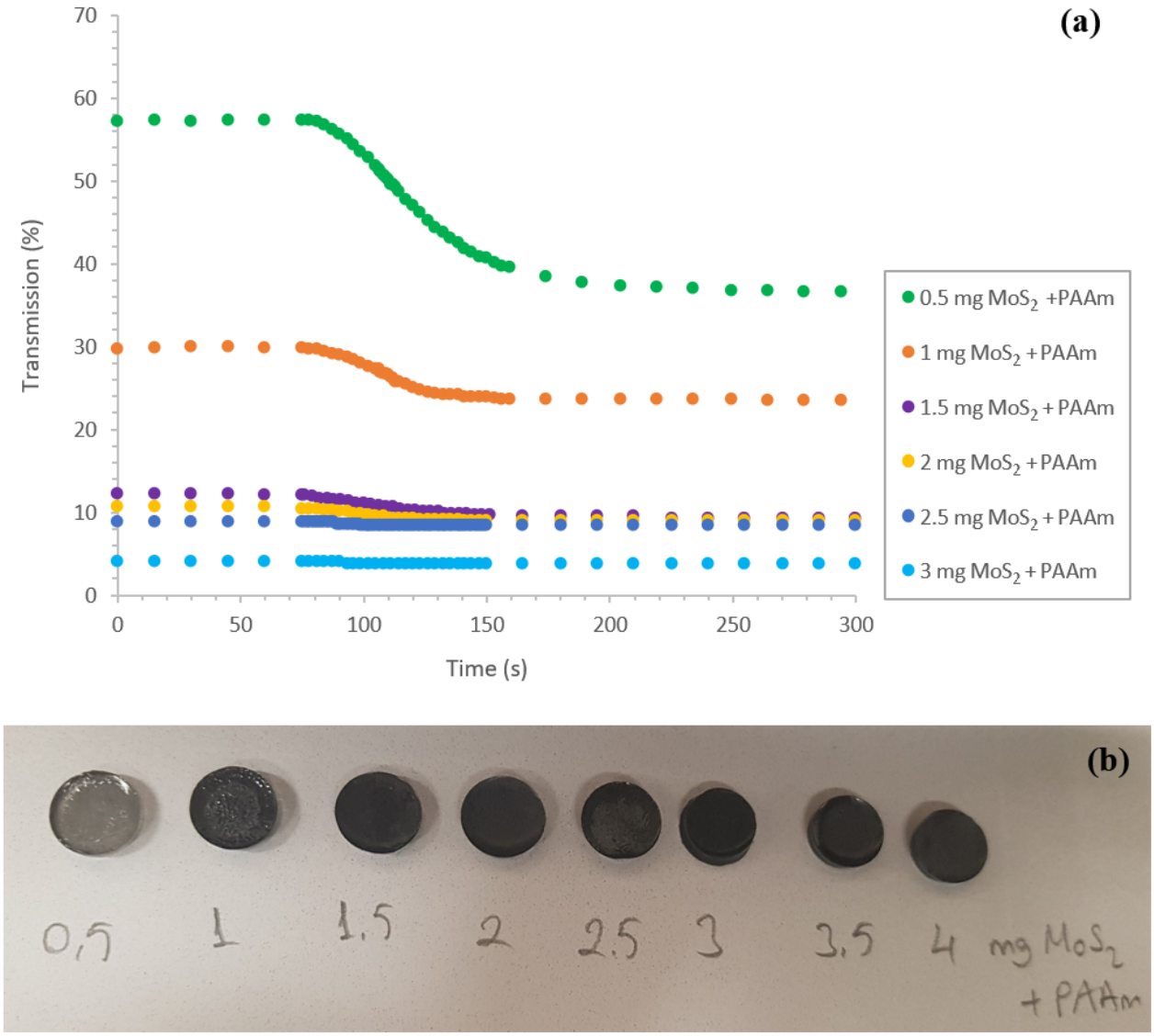

Figure 1. **(a)** Transmission-time graph of light through MoS_2-PAAm solutions with different MoS_2 amounts inside a quartz cuvette. These spectra are used to obtain the sol-gel transition points of different polymer composites. **(b)** Dried MoS_2-PAAm composite discs with various MoS_2 contents.

the gel decreases due to the new scattering centers formed by the microgels that increase with the monomer consumption, supporting Eq. (2.3). The difference between the largest and smallest values of the transmission values decreases as the amount of MoS_2 in the composite solution increases. Therefore, as the amount of MoS_2 in the composite increases, it becomes difficult to determine the difference between the minimum and maximum transmission response of the composite material and the gel point. As a matter of fact, it was noted that the transmission percentage values of composites containing 3.5 and 4 mg MoS_2 were in the range of $2.0\% - 2.2\%$ and $0.2\% - 0.3\%$, respectively; therefore, the measurement results of these composites are not included in Figure 1a. Figure 1b shows all composites left to dry for 1 week in a beaker at room temperature and in an open laboratory

environment. It is seen that PAAm composites with high MoS_2 doping almost do not transmit light. This confirms the measurement results given in Figure 1a.

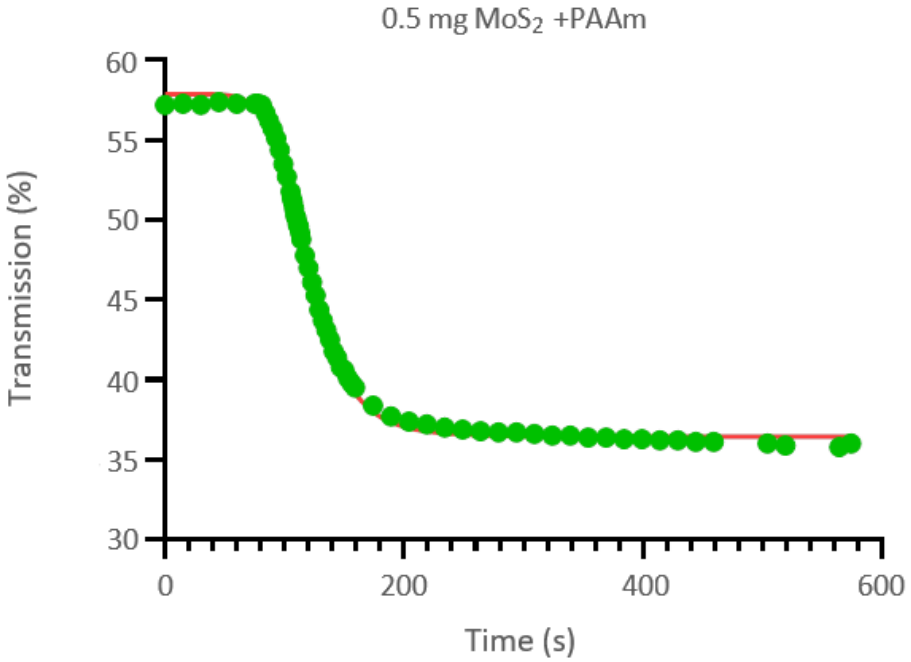

Figure 2. NUV-Vis transmission of MoS_2-PAAm composite with 0.5 mg of MoS_2 at 650 nm wavelength.

The nonlinear fitting of each curve gives a special transition point, namely gel point which corresponds to the time of geometrical phase transition from sol to gel for each polymer composite. As a result of the nonlinear fitting of the curves using the `GraphPad Prism 9.4.1` program, the best fitting function (R squared value closest to 1) was found to be Sigmoidal 4PL, X Concentration. The formula for this function can be given as follows:

$$y = b + x^h(t - b)/(x^h + t_g^h) \tag{4.1}$$

Here, t (Top) and b (Bottom) are the plateaus in the units of the y-axis. h (HillSlope) describes the steepness of the family of curves. A HillSlope of 1.0 is standard, and one should consider constraining the HillSlope to a constant value of 1.0. A HillSlope greater than 1.0 is steeper, and a HillSlope less than 1.0 is shallower. In this case, t_g is the gel point which represents the transition from sol to gel. For polymer composite obtained by adding 0.5 mg MoS_2 into 5 ml polyacrylamide solution, the transmission graph (green data points) measured by UV-Vis spectrophotometer and the fitting result (red line) made with the `GraphPad Prism 9.4.1` program are given in Figure 2. The fitting results of the transmission-time graphs of polymer composites doped with other MoS_2 amounts were obtained. The fitting parameters and the MoS_2-content-dependent gel point, t_g values of the composites are listed in Table 1. Figure 3 depicts the tendency of acceleration of gelation process when MoS_2 content is increased.

Table 1. The fitting parameters and the MoS_2-content-dependent gel point, t_g values of the composites.

MoS_2 content (mg)	**0.5**		**1**		**1.5**		**2**		**2.5**		**3**	
Best-fit values		**Range**		**Range**		**Range**		**Range**		**Range**		**Range**
b (Bottom)	36.43	36.30 to 36.58	23.56	23.52 to 23.61	9.403	9.389 to 9.416	8.908	8.889 to 8.927	8.45	8.428 to 8.467	3.821	3.712 to 3.954
t (Top)	57.89	57.55 to 58.08	29.9	29.79 to 29.94	12.22	12.19 to 12.24	10.63	10.60 to 10.65	8.825	8.790 to 8.851	4.011	3.983 to 4.021
t_g	120.1	119.5 to 121.0	117.1	116.7 to 117.6	106.1	105.5 to 106.7	100.2	99.5 to 101.2	97.4	95.2 to 99.7	95.5	92.8 to 97.2
h (HillSlope)	-6.82	-7.140 to -6.618	-10.45	-11.08 to -10.07	-6.613	-6.832 to -6.432	-7.951	-8.451 to -7.571	-8.678	-12.35 to -6.413	-9.224	-10.352 to -9.043
Goodness of Fit												
Degrees of Freedom	60		50		53		37		89		48	
R squared	0.998		0.9985		0.9991		0.9978		0.9153		0.9541	
Sum of Squares	6.77		0.449		0.055		0.0358		0.1078		0.0572	
Sy.x	0.336		0.0948		0.0322		0.0311		0.0348		0.0337	
Number of points analyzed												
# X values	64		54		57		41		93		52	
# Y values	64		54		57		41		93		52	

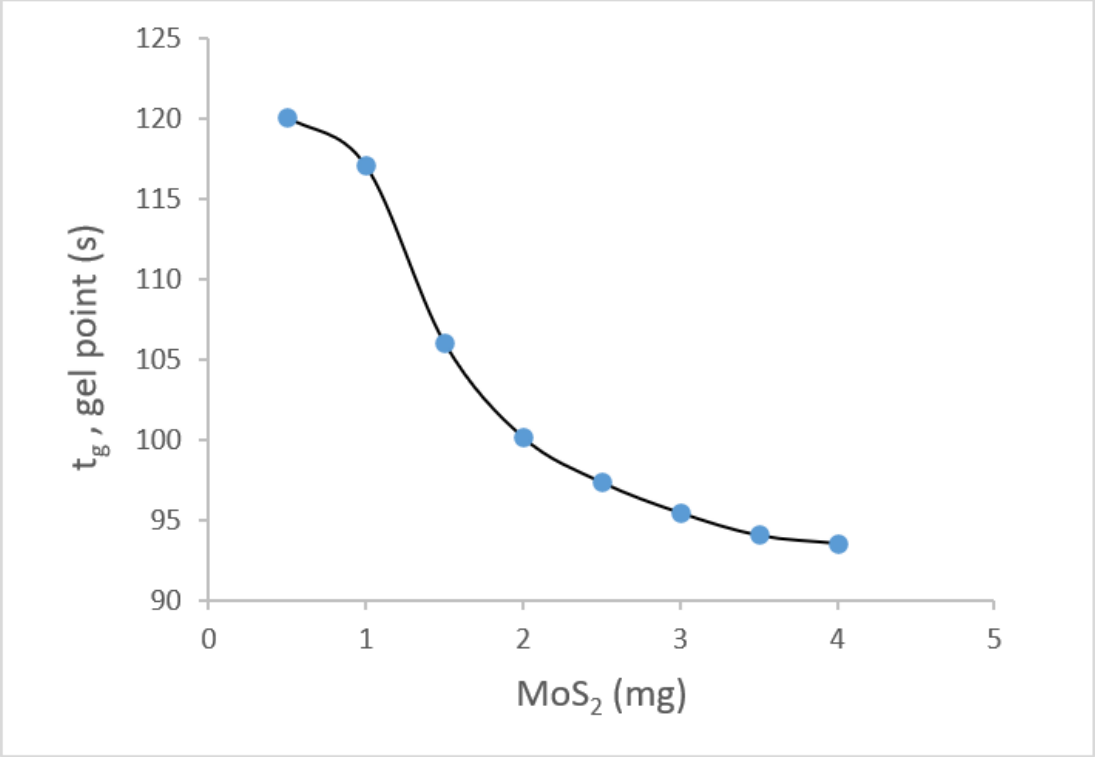

Figure 3. Determined gel point versus MoS_2 content graph.

The light with a constant wavelength in visible region coming to the solution in the quartz cuvette, passes through the solution easily in a transparent medium with only PAAm, while passing through the PAAm composite solution doped with a low amount of MoS_2, it is scattered by certain two-dimensional scattering centers, and while some of it passes through the solution, a negligible amount is absorbed. However, scattering and absorption are expected to be more effective in light coming into a dense composite solution (dispersive medium) with a large amount of MoS_2. Figure 4 is created by calculating the scattering intensity from the transmission data measured at 30 s intervals (45, 75, 105, 135, 165 s) before and after the sol-gel transition point, also taking into account the absorption. In Figure 4, the y-axes in the graphs were plotted using data normalized to the maximum value of scattering intensity they have. When the amount of MoS_2 in the composite is 2.5 mg, the scattering intensity is as high as possible and remains constant for larger amounts.

Scattering caused by the microgel and water in the composite material contributes to the opacity of the material. However, the low scattering intensity resulting from pregelation microgels increases with macrogel formation after gelation. The graphs of scattering intensity depending on the amount of MoS_2 given in Figure 4 were also found to be compatible with the theoretical approach. As the amount of MoS_2 in the composite gel increased, a shift towards lower time in the gel point (earlier gelation) was observed.

For a composite gel, considering that the microgel concentration is proportional to the amount of MoS, the scattering intensity can be written as fractal size as a function of the amount of MoS_2:

$$I_{sc} = (MoS_2)^d. \tag{4.2}$$

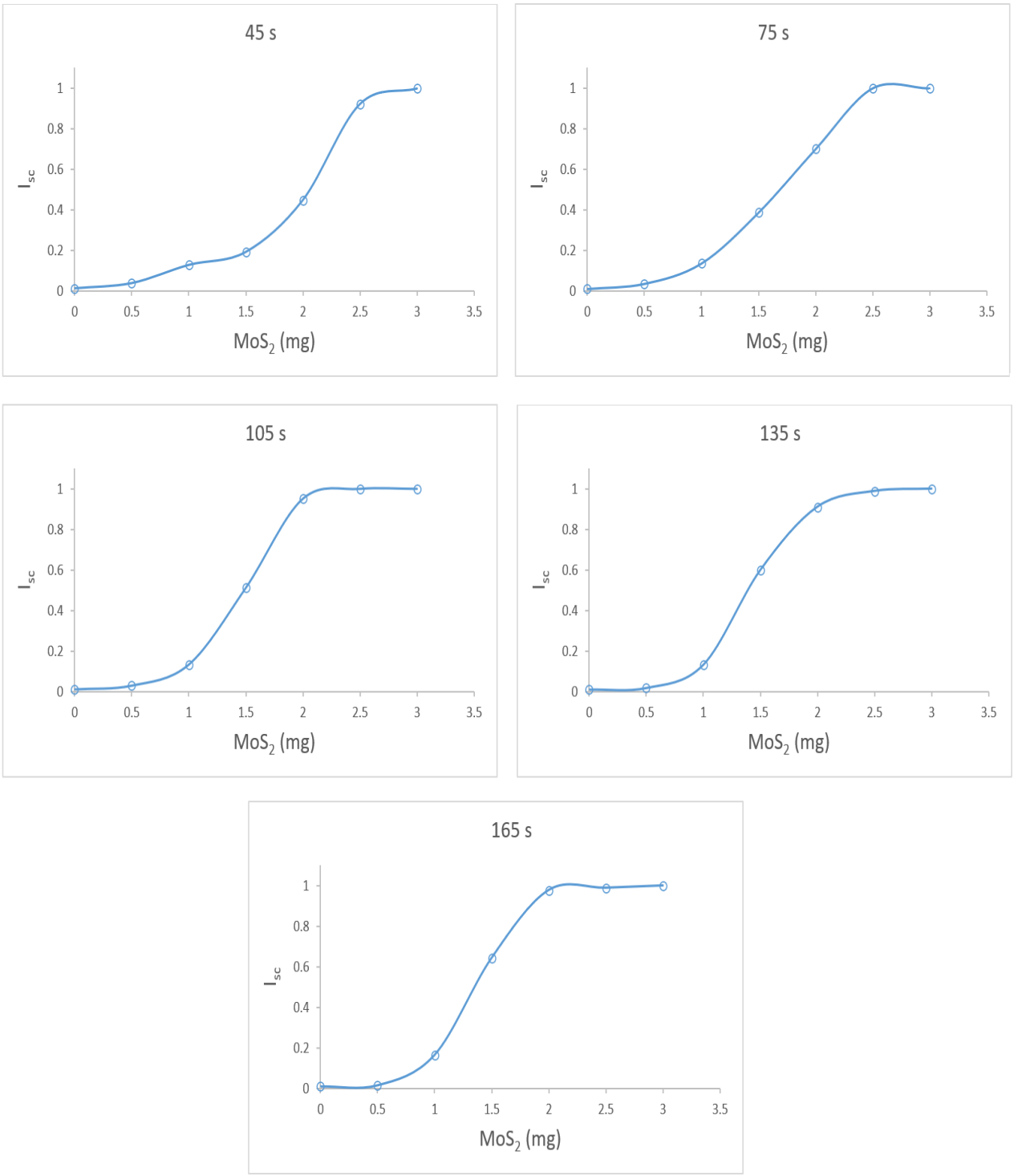

Figure 4. The plots of the scattering intensities, I_{sc} versus MoS_2 content at various times (45, 75, 105, 135, 165 s).

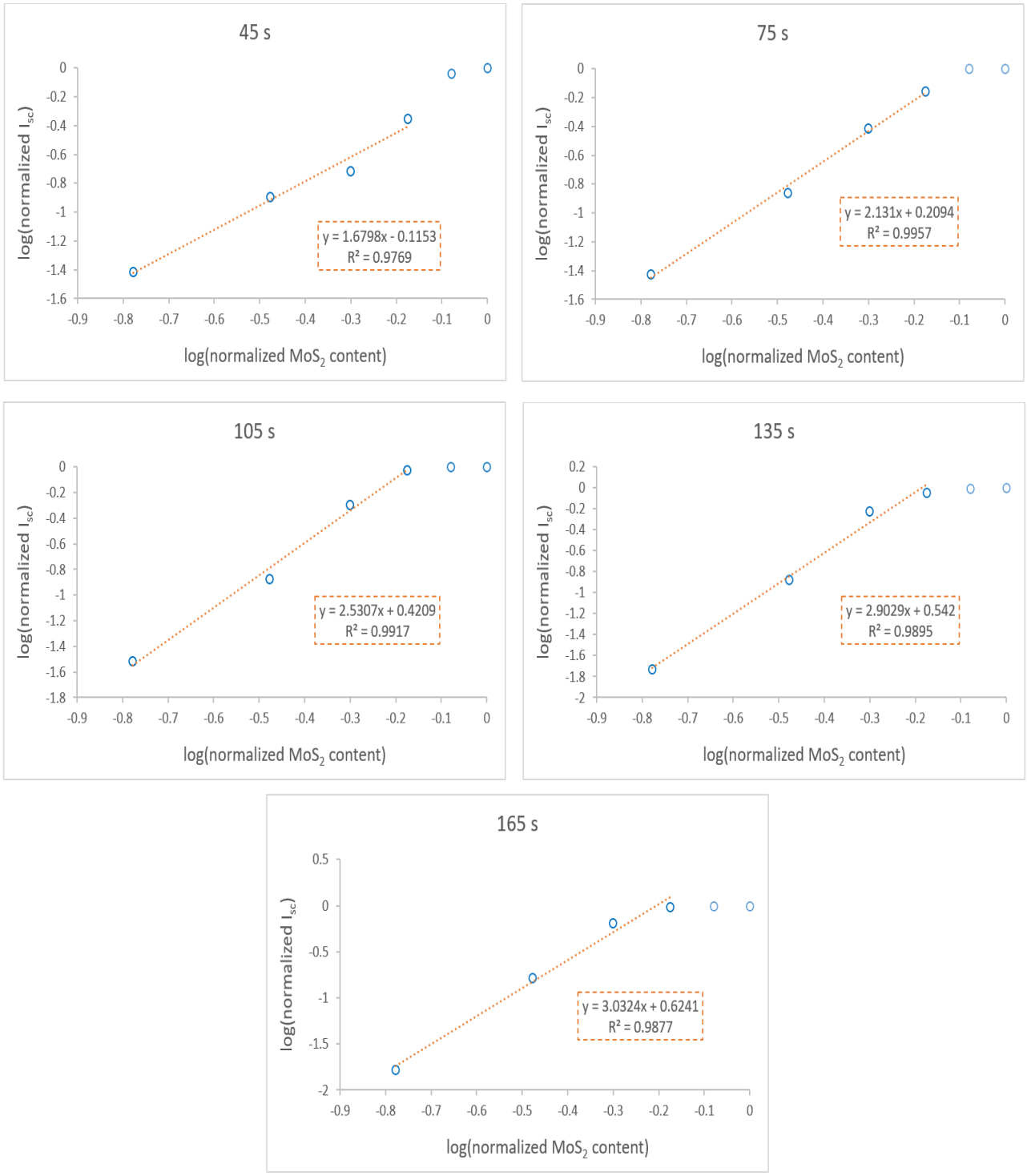

Figure 5. Log-Log plots of normalized I_{sc} versus MoS_2 content for various times (45, 75, 105, 135, 165 s). The coefficient, which is the multiplier of x, gives the slope of the line obtained by fitting each graph. These slopes yield the fractal dimensions of composites.

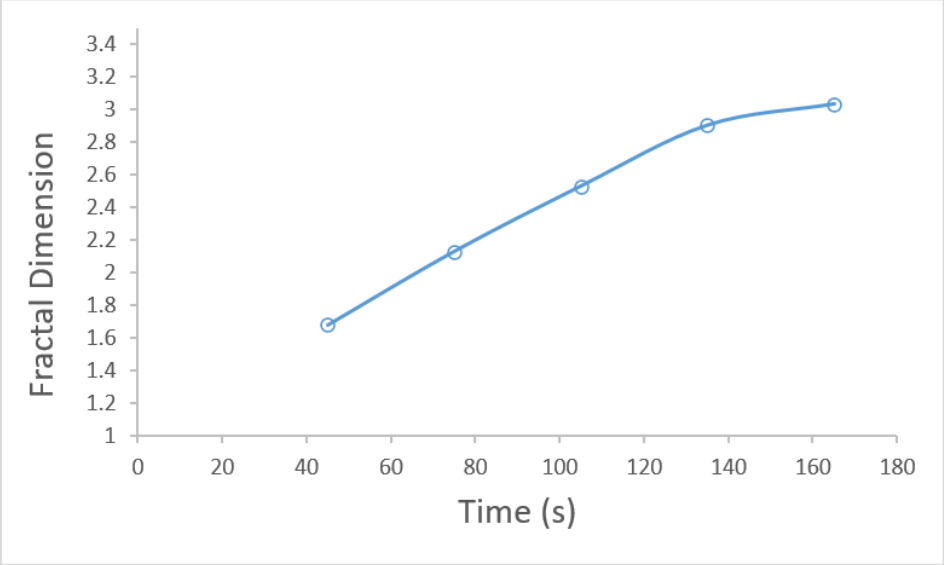

Figure 6. The plot of the fractal dimension versus time.

Figure 5 is created to calculate the fractal dimension, which is the exponential term in Eq. (4.2). Log-Log graphs of normalized I_{sc} versus MoS_2 content for various times (45, 75, 105, 135, 165 s) are given in Figure 5. The coefficient, which is the multiplier of x, gives the slope of the line obtained by fitting each graph. These slopes yield fractal dimensions. Calculated fractal dimension values are given in Figure 6 as a function of time. After about 105 s, the fractal size was found to be 2.53. This value is almost the same as 2.52, which represents a 3D percolation cluster [28, 29]. With the inclusion of more MoS_2s in the composite system, the number of empty spaces gradually decreases, and finally, it is observed that the fractal dimension approaches 3 for the highest MoS_2 amounts and the 3-dimensional structure is fully revealed.

5. Conclusion

The characteristics of the new composite material formed by doping MoS_2 (2D material) into PAAm polymer are investigated. Experimental results are elaborated regarding the gel point, compactness of the gel network, and gelation based on theory of Flory-Stockmayer, and other assumptions in the literature. Decrement in transmitted photon intensity is observed for all samples after a certain time, called gel point, t_g. Here it is seen as MoS_2 content is increased, t_g values decreased, presenting the acceleration in gel formation, most probably MoS_2 structures promote the polymerization reaction of AAm monomers with Bis. It is understood that inclusion of MoS_2 in PAAm system during sol-gel transition contributes to increasing the gelation process by increasing the rate of polymerization. Besides, more compact PAAm gels are produced in the presence of MoS_2 structure. A tendency of heterogeneity inside the polymer composite system is associated with this behavior. Inclusion of MoS_2 causes high intramolecular crosslinking and affects compactness of the composites. Microgels are located at the junction points of the Cayley tree. It was found that there is an increase in fractal dimension of composites from 1.67 to 3.03 with time. Fractal dimension is 2.53 for the intermittent percolation cluster formation around gel point which indicates that there is a 3D percolation cluster

formation after 105 s. As the amount of MoS_2 increases in the polymer composite, the empty spaces begin to fill and percolation occurs throughout the tree structure, and finally, the formation of 3D structure is observed. The fact that the fractal dimension has a value close to 3 for high MoS_2 amounts confirms this assumption. For future work, in addition to this study, calculations of fractal dimensions can be repeated for more data obtained by performing similar measurements for MoS_2 in different amounts between 0.5 mg and 1.5 mg. It was also confirmed that hydrogels formed rapidly within seconds. This indicates that a 3D network is formed within the gel. Due to this highly desirable 3D self-organizing property, these materials have great potential for wearable and embedded electronics.

References

[1] A. K. Geim, "Graphene: Status and Prospects," *Science* **324** (2009) 1530.

[2] M. Chhowalla, H. S. Shin, G. Eda, L. J. Li, K. P. Loh et al., "The chemistry of two-dimensional layered transition metal dichalcogenide nanosheets," *Nat. Chem.* **5** (2013) 263.

[3] B. Radisavljevic, A. Radenovic, J. Brivio, V. Giacometti, A. Kis, "Single-layer MoS_2 transistors," *Nature Nanotechnology* **6** (2011) 147.

[4] W. Z. Wu, L. Wang, Y. Li, F. Zhang, L. Lin et al., "Piezoelectricity of single-atomic-layer MoS_2 for energy conversion and piezotronics," *Nature* **514** (2014) 470.

[5] R. M. Navarro Yerga, M. C. A. Galván, F. del Valle, J. A. V. de la Mano, J. L. G. Fierro, "Water Splitting on Semiconductor Catalysts under Visible-Light Irradiation," *Chem. Sus. Chem* **2** (2009) 471.

[6] K. Maeda, "Photocatalytic water splitting using semiconductor particles: History and recent developments," *J. Photochem. Photobiol.* **12** (2001) 237.

[7] S. M. Notley, "High yield production of photoluminescent tungsten disulphide nanoparticles," *Journal of Colloid and Interface Science* **396** (2013) 160.

[8] B. Dey, R. K. Mondal, S. Mukherjee, B. Satpati, N. Mukherjee et al.,, "A supramolecular hydrogel for generation of a benign DNA-hydrogel," *RSC Advances* **5** (2015) 105961.

[9] S. Dhibar, A. Dey, D. Ghosh, A. Mandal, B. Dey, "Mechanically tuned molybdenum dichalcogenides (MoS_2 and MoSe2) dispersed supramolecular hydrogel scaffolds," *Journal of Molecular Liquids* **276** (2019) 184.

[10] I. Y. Jeon, J. B. Baek, "Nanocomposites Derived from Polymers and Inorganic Nanoparticles," *Materials.* **3** (2010) 3654.

[11] E. Arda, S. Kara, Ö. Pekcan, G. A. Evingür, "Evaluation of the fractal dimension of polyacrylamide during gelation and swelling," *Materials Today Communications* **26** (2021) 101980.

[12] S. Kara, E. Arda, F. Dolastir, Ö. Pekcan, "Electrical and optical percolations of polystyrene latex–multiwalled carbon nanotube composites," *Journal of Colloid and Interface Science* **344** (2010) 395.

[13] E. Arda, Ö. B. Mergen, Ö. Pekcan, "Electrical and optical percolations in PMMA/GNP composite films," *Phase Transitions* **91** (2018) 546.

[14] Ş. Uğur, Ö. Yargı, Ö. Pekcan, "The chemistry of two-dimensional layered transition metal dichalcogenide nanosheets," *Procedia Engineering* **10** (2011) 1709.

[15] T. Krasian, W. Punyodom, P. Worajittiphon, "A hybrid of 2D materials (MoS_2 and WS_2) as an effective performance enhancer for poly(lactic acid) fibrous mats in oil adsorption and oil/water separation," *Chemical Engineering Journal* **369** (2019) 563.

[16] S. Voyutsky, "Colloid Chemistry," Mir Publishers, Moscow, (197) 38.

[17] R. J. Young, "Introduction to Polymers," Introduction to Polymers, New York, (1983).

[18] P. J. Flory, "Molecular size distribution in three dimensional polymers. I. Gelation," *Journal of the American Chemical Society* **63** (1941) 3083.

[19] W. H. Stockmayer, "Theory of molecular size distribution and gel formation in branched-chain polymers," *The Journal of Chemical Physics* **11** (1943) 45.

[20] D. Stauffer, A. Coniglio, M. Adam, "Gelation and critical phenomena," In: Dušek, K. (eds) Polymer Networks, *Advances in Polymer Science,* **44** (1982) 103.

[21] D. Stauffer, "Introduction to Percolation Theory," Taylor & Francis London (1985).

[22] H. J.Herrmann, "Geometrical cluster growth models and kinetic gelation," *Physics Reports* **136** (1986) 153.

[23] D. G. De Gennes, "Scaling Concepts in Polymer Physics," Cornell University Press, Ithaca, USA (1988).

[24] D. K. Aktaş, G. A. Evingür, Ö. Pekcan, "Critical exponents of gelation and conductivity in polyacrylamide gels doped by multiwalled carbon nanotubes," *Composite Interfaces* **17** (2010) 301.

[25] J. P. Cohen Addad, "NMR and fractal properties of polymeric liquids and gels," *Progress in Nuclear Magnetic Resonance Spectroscopy* **25** (1993) 1.

[26] L. Pietronero, E. Tosatti, "Fractals in Physics," Elsevier Science Publishers B.V, North Holland, (1986).

[27] D. W. Schaeffer, K. D. Keefer, "Fractal Aspects of Ceramic Synthesis," *MRS Online Proceedings Library* **73** (1986) 277.

[28] M. Sahimi, "Applications of Percolation Theory," CRC Press, London, (2003).

[29] D. Stauffer, A. Aharony, "Introduction To Percolation Theory," Taylor and Francis, London, (1994).